

# Implementation of Orthogonal Frequency Coded SAW Devices Using Apodized Reflectors

Derek Puccio, Don Malocha, Nancy Saldanha  
Department of Electrical and Computer Engineering  
University of Central Florida  
Orlando, FL 32816-2450  
rick.puccio@ieee.org

**Abstract**—Recently, orthogonal frequency coding (OFC) has been presented as a novel method for coding SAW tags and sensors [1]. Orthogonal frequency coding is a spread spectrum technique and has been shown to provide enhanced processing gain and reduced time ambiguity resulting in greater range and increased sensitivity when compared with single carrier frequency devices. The sensor works both as a tag and a sensor with the ability to send back “tagged” sensor information in a multi-sensor environment. The tag information is provided by a series of reflectors which map into a known chip sequence. The time-chip- sequence is coded by differing OFC and PN sequences. Therefore, the implementation of an OFC sensor requires reflectors having differing local carrier frequencies. In the case of narrow fractional bandwidths or high reflectivity (such as on LiNbO<sub>3</sub>), it is desirable to adjust the reflectivity per electrode in the various chips.

For varying system requirements, the use of weighted reflectors is an option; both apodization and variable weighted reflectors are investigated. Experimental results on cosine weighted apodized reflectors will be compared to COM predictions on YZ LiNbO<sub>3</sub>.

This paper presents several OFC SAW device embodiments that are employed using wideband input transducers and multiple weighted reflector gratings. The devices operate in the differential mode using gratings on either side of the transducer. The advantages of using the weighted reflector gratings in OFC SAW devices are discussed. OFC temperature sensor device experimental results are presented using weighted reflectors to obtain the proper time coded response and compared to predictions.

## I. INTRODUCTION

Orthogonal frequency coding (OFC) is a spread spectrum coding technique that has been successfully applied to SAW tags and sensors [2]. OFC offers several advantages over single frequency SAW tags and sensors including enhanced processing gain, increased range using chirp interrogation, and improved security. In addition, OFC relies on the use of

several frequencies making simultaneous sensing and tagging possible in multiple sensor environments. OFC SAW devices are implemented using reflectors with periodicities chosen to match the chip frequency of interest. As a result, an OFC SAW device contains a series of reflectors whose center frequencies correspond to the OFC signal of interest. In the case of high reflectivity or narrow bandwidth materials, it is desirable to control the reflection and transmission characteristics of each reflector. The goal of this research is to study weighted reflectors as a method of controlling the reflected and transmitted SAW energy. In addition, arbitrary pulse shapes can be achieved using reflector weighting. Furthermore, pulse shaping can be used in phase shift keying, such as in phase and quadrature channels in minimum shift keying (MSK).

Several steps must be taken in order to properly implement weighted reflectors. Both withdrawal weighting and apodization result in structures that contain various metallized and free surface regions. As a result, an accurate description of SAW velocity within these regions is critical to successful reflector design. Experimental velocity results as a function of normalized metal thickness and reflector duty cycle are given, and a discussion of the results is provided. Additionally, a two dimensional COM model has been created for analysis and design of apodized reflectors, and experimental results are compared with predictions for cosine weighted reflectors. Finally, experimental and simulated responses of an OFC SAW sensor using cosine weighted reflectors are given. The responses are applied to a simulated transceiver and results are discussed.

## II. REVIEW OF OFC TAGS AND SENSORS

Orthogonal frequency coding (OFC) makes use of orthogonal frequencies in a manner similar to M-ary FSK. The orthogonality integral requires a relationship between local chip frequencies and their bandwidths. An example of a signal utilizing orthogonal frequencies is the linear stepped chirp shown in Figure 1. Each of the seven chips has a unique carrier center frequency as indicated by the individual

---

This work is supported by the Florida Solar Energy Center (FSEC) and NASA. D. Puccio is supported by the NASA Graduate Student Researcher's Program (GSRP).

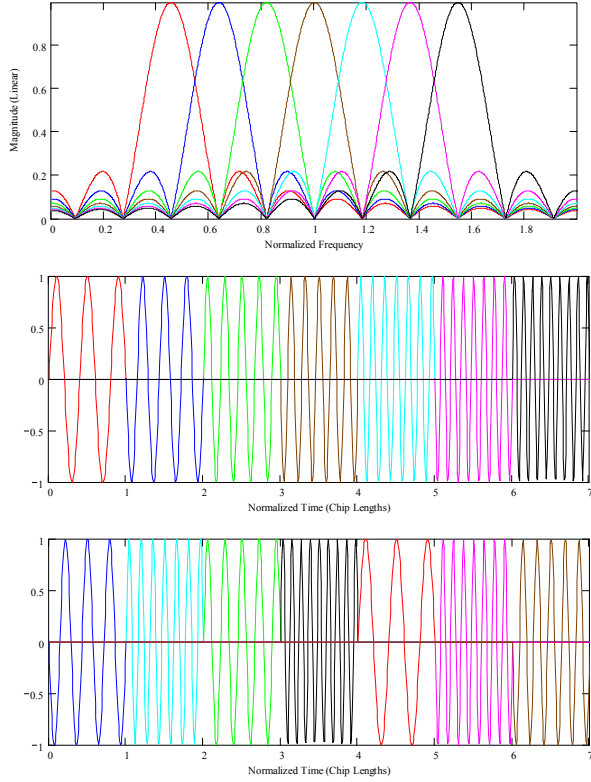


Figure 1. Example of OFC uniform chip frequency responses (upper), stepped chirp response (middle), orthogonal frequency coded waveform (lower)

chip frequency responses also shown in Figure 1. The frequency responses indicate that the center frequency of each chip is coincident with nulls of all other chip frequency responses. A level of coding is achieved by shuffling the chips so that the local carrier frequencies are no longer contiguous in time as shown in Figure 1. The order in which the orthogonal frequencies are used determines the code. The coded signal and the linear stepped chirp occupy the same bandwidth and all coding information is contained within the signal phase.

OFC can be applied to SAW tags and sensors using shorted periodic reflector gratings as shown in Figure 2. Each reflector's periodicity is chosen so that the reflector center frequency corresponds to the OFC chip of interest. The device schematic shown is that of a temperature sensor which uses identical reflector banks on either side of a wideband transducer. However, different free space delays are employed on each side of the transducer. The impulse response of this device contains two identical approximations of the OFC signal of interest as shown in Figure 2. During matched filtering, this device produces two compressed pulses. The separation between the pulses is proportional to device temperature.

### III. SAW VELOCITY EXTRACTION

Weighted reflectors can be employed using withdrawal weighting or apodization. Both techniques rely on

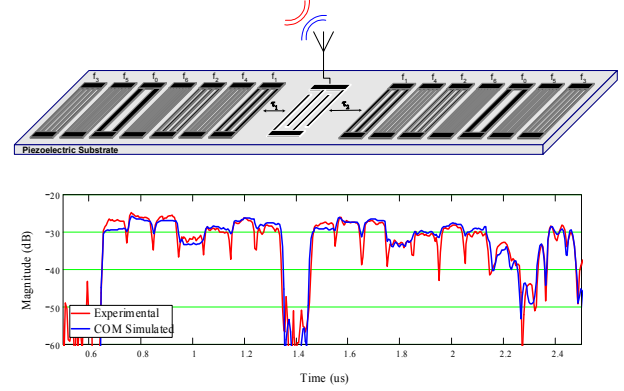


Figure 2. Orthogonal frequency coded SAW temperature sensor schematic (upper) and sensor impulse response (lower).

eliminating portions of the metallized surface used in a uniform reflector. As a result, weighted reflector designs must account for velocity perturbations in order to keep wave fronts from different sections of the reflector phase coherent. For this reason, reflector velocity data were extracted for YZ LiNbO<sub>3</sub>.

Reflector velocities were extracted using the following equation derived from a transmission line model analogy [3].

$$v_g \left( \frac{h}{\lambda}, \frac{a}{p} \right) = v_{fs} \cdot \left[ 1 + \frac{a}{p} \cdot \frac{\Delta v}{v_{fs}} - \frac{1}{\pi} \cdot \frac{B_0}{Y_0} \sin \left( \frac{a}{p} \right) \right] \quad (1)$$

where,  $v_{fs}$  = free surface velocity

$\frac{a}{p}$  = reflector grating duty cycle

$\frac{h}{\lambda}$  = normalized metal thickness

This equation is a function of two independent variables, the reflector grating duty cycle and normalized metal thickness. The difference between metallized and free surface velocities,  $\Delta v$ , is proportional to the normalized metal thickness. The transmission line model uses a shunt susceptance term,  $B_0/Y_0$ , to account for stored energy at the front and back of each reflector electrode, and this term is proportional to the square of the normalized metal thickness.

The unknown terms in (1) were extracted using a test mask with several test structures. The test devices used a simple delay line with a reflector grating situated nearby. This embodiment is used in order to isolate just the reflector response using signal processing [3]. The test mask contained thirty five of these devices each having different combinations of reflector grating duty cycle and center frequency wavelength. Seven wavelengths were used between 18 and 60  $\mu\text{m}$ , and five reflector grating duty cycles between 40% and 60% were employed. The mask was fabricated on YZ LiNbO<sub>3</sub>, and signal processing techniques were applied to the swept frequency responses to extract reflector grating velocity data. A three dimensional optimization was performed using these data in order to obtain the unknown terms in (1). The results for several metal thicknesses are shown in Figure 3, and there is good

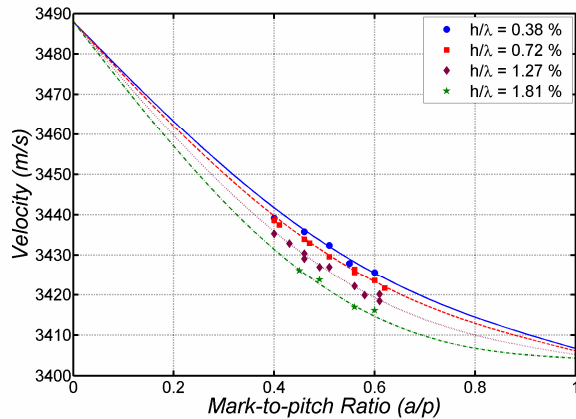


Figure 3. YZ LiNbO<sub>3</sub> velocity vs. reflector duty cycle for several normalized metal thicknesses. Curvature increases with metal thickness due to stored energy at edges of electrodes.

agreement between measured and predicted results. Note that the curvature of each line is proportional to the normalized metal thickness. This is a direct result of the stored energy effect which has a large influence for thicker films.

#### IV. WEIGHTED REFLECTORS

##### A. Reflector Weighting Techniques

Reflector weighting can be accomplished using withdrawal weighting or apodization. Previous studies of withdrawal weighting focused on eliminating unwanted modes in resonant cavities by shaping reflector frequency responses [4,5,6]. For OFC tag and sensor applications, the time domain response is of primary concern, and is better approximated through apodization. Therefore, the goals of this research are simulation and implementation of apodized reflectors.

##### B. Implementation of Apodized Reflectors

In an apodized reflector, each electrode covers a portion of the beam aperture defined by a sampled time window. As an example, Figure 4 shows a schematic of a sixteen period cosine weighted reflector. Note that the first eight electrodes are connected to the bottom bus bar, and the rest are connected at the top. This is done in order to reduce group delay variations over the reflector aperture. In order to simulate such a device, a two dimensional COM model was developed. The model is designed to segment the beam aperture in to uniform tracks as shown. The sum of each track's swept frequency response yields the overall reflector response.

When designing apodized reflectors, special care must be taken to ensure phase coherence of the reflected waves from different tracks. As an example, consider an incident wave on the left side of the reflector shown in Figure 4. A portion of the wave will be reflected from track *A*, and after a short delay, another portion is reflected from

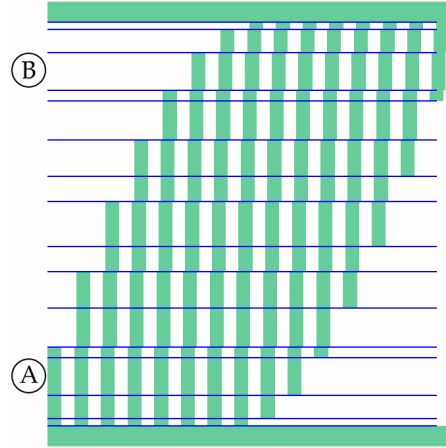


Figure 4. Schematic of cosine weighted apodized reflector. Reflector is simulated by creating uniform tracks and summing responses from each.

track *B*. This delay is implemented using a free surface which has a slightly higher velocity than within the electrodes. As a result, if no correction is made, the reflected waves from tracks *A* and *B* will have a small phase difference. Therefore, the initial free space delays must be extended slightly in order to keep the reflected waves coherent. The resulting electrodes will be made up of several smaller rectangles that are staggered across the aperture as shown.

##### C. Cosine Weighted Reflector Results

Using the apodization technique described, a weighted reflector was designed and fabricated using a cosine window for operation on YZ LiNbO<sub>3</sub> at 250 MHz. The reflector contained 24 periods, and was placed near a simple delay line as in [3]. The device's swept frequency response was obtained and signal processing applied in order to isolate the reflector response. The device was also simulated using the 2-D COM model, and the simulated and experimental reflector responses are plotted in Figure 5. Overall, there is good agreement between the simulated and predicted responses. However, the experimental response is nonsymmetrical, and has wider bandwidth than the prediction. To gain a better understanding of the differences between the simulated and measured reflector responses, an FFT was applied to both. In Figure 6, the time domain responses reveal that the experimental reflector response is shorter than the simulated which

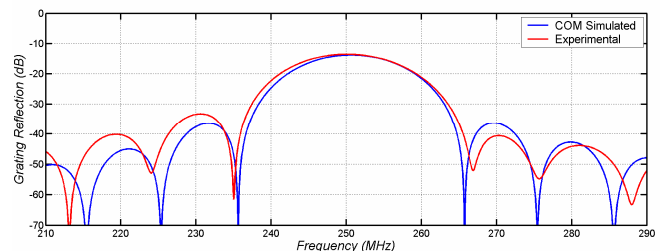


Figure 5. 2-D COM simulated and experimental responses of 24 period cosine weighted apodized reflector on YZ LiNbO<sub>3</sub>.

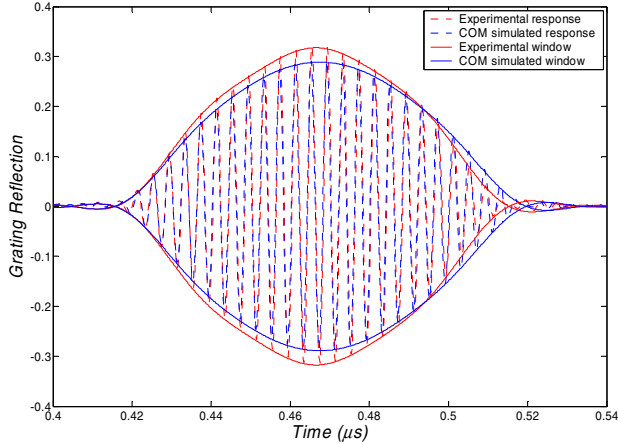


Figure 6. 2-D COM simulated and experimental cosine weighted reflector time domain responses. Experimental response has shorter duration due to velocity errors.

is expected due to the difference in their bandwidths. It is believed that the errors are caused by phase differences of the reflected waves from each track of the reflector. This result underlines the importance of accurate velocity information when designing weighted reflectors.

## V. OFC TEMPERATURE SENSOR USING COSINE REFLECTORS

Implementation of an OFC SAW temperature sensor was accomplished using cosine weighted reflectors. Previous studies have defined a set of orthogonal frequencies for uniform weighting [1,2]. Using a similar approach, orthogonal frequencies can be defined for several window types. Orthogonal frequencies for cosine weighting are defined as  $f_n = 2 \cdot n \cdot \tau^{-1}$ . Using this definition, a cosine weighted OFC temperature sensor was designed for operation on YZ LiNbO<sub>3</sub>. The sensor was implemented using three cosine weighted reflectors as shown in Figure 7, and occupied a 24.5% fractional bandwidth centered at 250 MHz.

The device was simulated using the 2-D COM model and verified by experiment using devices fabricated on YZ LiNbO<sub>3</sub>. The simulated and experimental responses have been transformed into the time domain using an FFT, and are shown in Figure 8. The plot shows the cosine weighted reflector responses from either side of the transducer, and there is good agreement between measured and predicted responses.

The experimental response was then applied to a simulated transceiver, and a compressed pulse response from one reflector bank is shown in Figure 9. The autocorrelation of the matched filter is also shown for comparison. Note the two pulses located one half chip length away on either side of the compressed pulse. These pulses are undesired, and subsequent calculations have shown that the level of these responses can be significantly reduced by implementing the device using in phase and quadrature channels along with PN coding. Lastly, the OFC sensor was tested over temperature

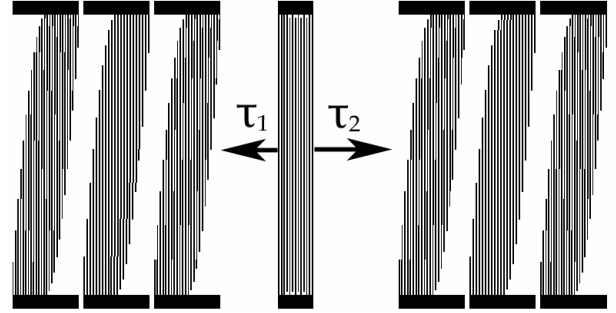


Figure 7. Schematic drawing of three chip cosine weighted OFC sensor. Identical weighted reflector banks are placed on either side of wideband transducer. Free space delays are not drawn to scale.

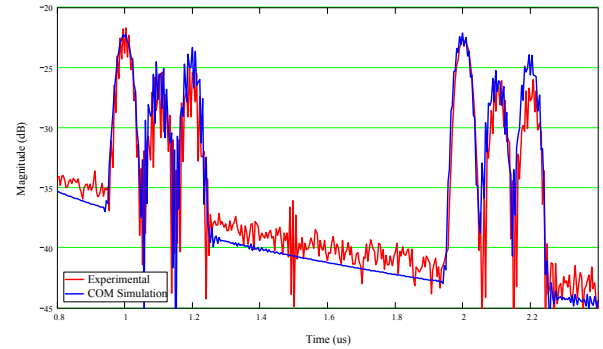


Figure 8. Simulated and experimental time domain responses of three chip OFC SAW temperature sensor. Sensor implemented using cosine weighted apodized reflectors.

between 10°C and 100°C, and the resulting compressed pulse responses are shown in Figure 10. Using an adaptive matched filter, the pulse amplitude remains constant as temperature is varied.

## VI. CONCLUSION

This paper demonstrated the use of weighted reflectors in orthogonal frequency coded SAW tags and sensors. A review of OFC was given, and its application to SAW tags and sensors was demonstrated. The importance of accurate SAW velocity information was discussed, and velocity profiles were extracted for YZ LiNbO<sub>3</sub>. A description of the extraction technique was given, and a discussion of the results was provided.

Reflector withdrawal weighting and apodization were both considered as weighting techniques, and apodization was chosen as the optimal method for weighting OFC SAW devices. A description was given of apodized reflector design criteria including correcting errors due to velocity perturbations. The final apodized reflector design was optimized to reduce group delay variations across the beam aperture and ensure phase coherence of the reflected waves from each uniform section of the reflectors. In addition, a two dimensional COM model was developed in order to properly simulate the apodized reflector designs.

The apodization design criteria were then applied to cosine weighted reflectors, and experimental devices

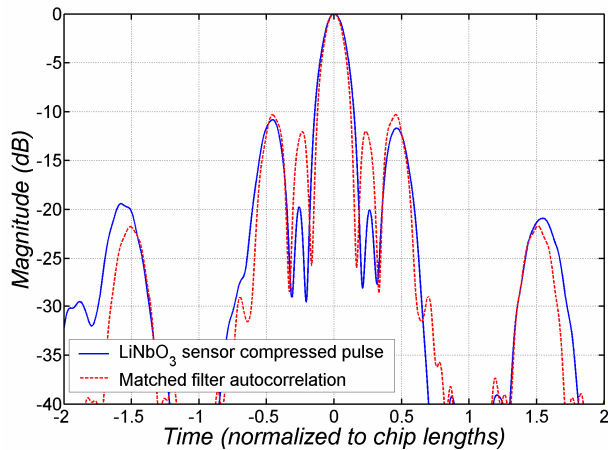


Figure 9. Compressed pulse response.

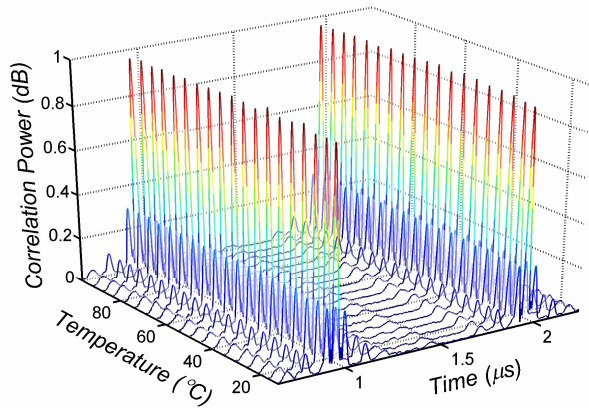


Figure 10. Cosine weighted OFC SAW sensor compressed pulses. Temperature varied between 10°C and 100°C. Adaptive matched filter yields uniform pulse amplitude as temperature varies.

fabricated on YZ LiNbO<sub>3</sub> were compared with simulated responses generated by the 2-D COM model. The simulated and experimental reflector responses were very similar; however, subsequent analysis revealed small errors due to phase differences of the reflected waves from each uniform track of the reflector. These errors revealed the importance of accurate material velocity information when designing weighted reflectors. Lastly, an OFC SAW temperature sensor was implemented using cosine weighted reflectors.

The 250 MHz OFC SAW sensor was fabricated on YZ LiNbO<sub>3</sub>, and its swept frequency response agreed well with 2-D COM model predictions. The sensor was then tested over temperature and the responses were applied to a simulated transceiver which uses an adaptive matched filter. Using the adaptive matched filter, results were given showing that the compressed pulse amplitudes remained constant as temperature varied.

The use of weighted reflectors for OFC sensors has been introduced, but additional work is warranted. Phase matching across the beam is difficult and more details need investigation to compensate exactly. Other weighting windows and embodiments may also show advantages for differing sensor applications.

#### ACKNOWLEDGMENT

The authors wish to thank NASA for supporting Derek Puccio through the Graduate Student Researcher's Program (GSRP). We also wish to thank the Florida Solar Energy Center (FSEC) and NASA for supporting this work. Our NASA point of contact is Dr. Robert Youngquist.

#### REFERENCES

- [1] D.C. Malocha, D. Puccio, D. Gallagher, "Orthogonal frequency coding for SAW device applications," *Proc. IEEE International Ultrasonics Symposium*, 2004, pp. 1082-1085.
- [2] D. Puccio, D.C. Malocha, D. Gallagher, J. Hines, "SAW sensors using orthogonal frequency coding," *Proc. IEEE International Frequency Control Symposium*, 2004, pp. 307-310.
- [3] P.V. Wright, "Modeling and experimental measurements of the reflection properties of SAW metallic gratings," *Proc. IEEE International Ultrasonics Symposium*, 1984, pp. 54-63.
- [4] T. Omori, J. Akasaka, M. Arai, K. Hashimoto, M. Yamaguchi, "Optimisation of weighted SAW grating reflectors with minimised time delay deviation," *Proc. IEEE International Frequency Control Symposium and PDA Exhibition*, 2001, pp. 666-670.
- [5] W.J. Tanski, "SAW resonators utilizing withdrawal weighted reflectors," *IEEE Transactions on Sonics and Ultrasonics*, Vol. 26, No. 6, pp. 404-410, November 1979.
- [6] P.D. White, R.F. Mitchell, R. Stevens, P. Moore, M. Redwood, "Synthesis and design of weighted reflector banks for SAW resonators," *Proc. IEEE International Ultrasonics Symposium*, 1978, pp. 634-638.